Thiourea Adsorbent for Efficient Removal of Mercury (II)

Claudine El Khoueiry, Fabrice Giusti, Evan Lelong, Guilhem Arrachart, Bilal Nsouli, Iyad Karame, Stéphane Pellet-rostaing

HAL Id: hal-04384786

https://hal.umontpellier.fr/hal-04384786

Submitted on 10 Jan 2024

ChemistrySelect

Research Article
doi.org/10.1002/slct.202303015

Chemistry Europe
European Chemical
Societies Publishing

www.chemistryselect.org

Thiourea Adsorbent for Efficient Removal of Mercury (II)

Claudine El Khoueiry,[a, c] Fabrice Giusti,[a] Evan Lelong,[a] Guilhem Arrachart,*[a] Bilal Nsouli,[b] Iyad Karame,[c] and Stéphane Pellet-Rostaing[a]

The removal of heavy toxic metals from industrial effluents is extremely important, especially for mercury (Hg), which is classified as a highly toxic even at low concentrations. For this purpose, novel thiourea chelating resins were synthesized as sorbent for Hg (II). Six different polymers of formo-phenolic types were characterized and evaluated for their chelating properties with respect to Hg (II) extraction. Batch adsorption studies of mercury (II) as a function of pH, initial metal ion concentration, temperature, and time showed that thiourea formo-phenolic polymers have a good affinity for Hg removal and a high adsorption capacity. Adsorption isotherms (Lang-muir and Freundlich) and kinetic models (pseudo-first and pseudo-second order) were used to interpret the sorption behavior of the materials. The Langmuir model yielded the best fit with a maximum adsorption capacity of 300 mg/g. Desorption studies were performed with aqueous thiourea solution and showed that the adsorbent is indeed regenerable and can be effectively used for up to three adsorption-desorption cycles with negligible loss of performance. This study confirmed the potential of thiol-modified formo-phenolic resins in sorbent engineering with promising applications in the remediation of mercury-contaminated water.

Introduction

One of the most serious environmental pollution problems is the discharge of heavy metals. These metals are classified as extremely hazardous elements.[1,2] The release of heavy metals such as Hg, Pb, Ni, Cd, Cu, and Zn into the environment has increased dramatically due to the rapid growth of industries such as metal plating facilities, mining, fertilizer industries, tannery, battery, paper, and pesticide industries, etc.[1,3,4] Usually, heavy metal ions are highly toxic, non-biodegradable, and accumulate in the environment and the living bodies.[5–7]

Among the heavy metals, mercury (Hg) occupies a prominent position in the list of high-priority elements set out in Directive 2008/105/EC of the European Parliament and of the Council of the European Union, which specifically addresses environmental quality standards in the field of water policy.[8] As per the guidelines set forth by the World Health Organization (WHO), the allowable concentrations of mercury should not exceed 1 μg/L in drinking water and 10 μg/L in industrial wastewater.[9,10] Mercury is mainly found in the aqueous phase in metallic form [Hg(II)] and organic form [MeHg] which are most toxic form of Hg.[11]

Prolonged exposure to mercury poses significant risks, including irreversible damage to the central nervous system, kidneys, reproductive organs, liver, and the potential for sensory and psychological disorders. These environmental and human safety problems occur at very low levels.[12–14]

The pollution related to this element continues to increase due to its widespread use or disposal in the industrial fields (telescopes, fluorescent lighting, dermatological therapy, etc.).[15] The most significant contamination is found in wastewater, which becomes contaminated. Consequently, addressing the presence of mercury in aquatic ecosystems has become an imperative global concern that requires urgent attention to protect public health. Therefore, the detection and removal of mercury from wastewater are crucial.[16–18]

Researchers have proposed several methods to remove heavy metals including mercury from wastewater in order to protect all living beings on earth and the environment.[16,19,20] Various methods have been described for this purpose, such as chemical precipitation,[21] ion exchange,[22] membrane filtration,[23] electrochemical treatment,[24] adsorption,[25] etc. These techniques have some drawbacks, such as low removal efficiency, unselectivity, high operating costs, large quantities of chemicals consumption and sludge generation.[26] Among the different methodologies proposed for mercury removal, the adsorption method is one of the most promising techniques due to its practical adaptability and cost-effective methodology coupled with its removal efficiency and recyclability of the adsorbents.[27–31]

Despite the widespread use of adsorption techniques, more efficient adsorbents are still being sought.[16,32]

A variety of adsorbents have been reported in the literature for the treatment of wastewater containing heavy metal ions, particularly Hg. These adsorbents include activated carbon,

[a] C. El Khoueiry, Dr. F. Giusti, Dr. E. Lelong, Dr. G. Arrachart, Dr. S. Pellet-Rostaing
ICSM, Univ Montpellier, CEA, CNRS, ENSCM, Marcoule, France
E-mail: guilhem.arrachart@umontpellier.fr

[b] Dr. B. Nsouli
Lebanese Atomic Energy Commission – National Council for Scientific Research Beirut, Lebanon

[c] C. El Khoueiry, Prof. I. Karame
Lebanese University, LCOM, Dept Chem, Faculty of Sciences I, Hadath, Lebanon

ChemistrySelect

Research Article
doi.org/10.1002/slct.202303015

Chemistry Europe
European Chemical
Societies Publishing

carbon nanotubes, polymers, zeolites, bio-adsorbents, and agriculture wastes.[3,20]

While adsorption is focused on developing novel adsorbents with fast kinetics, high adsorption capacity, selectivity and recyclability, natural materials are generally limited in meeting these requirements.[33] As a result, there is a strong interest in functional materials to address these challenges. Among them, chelating resins have been widely used due to their strong affinity and selectivity for heavy metal ions as well as their high physical and chemical stability.[34–36] Chelating resins have the advantage of incorporating a wide variety of ligands. The insertion of this chelating ligand allows them to be selective and efficient for the adsorption of a specific metal ion.[30,34,37] The adsorption selectivity of chelating resins depends on the ligand atoms: O, N, S and P according to Person Hard and Soft Acids and Bases (HSAB) theory.[38,39] Sulfur-containing ligands are more selective for the soft acid Hg (II) than their nitrogen and oxygen analogues because they form stronger complexes with it.[3] In addition, Hg (II) has an affinity for sulfur related to that Hg being a typical soft base and sulfur being a soft acid.[3,6,17] Meeting these properties, thioureas, known as sulfur analogues of carbamides, are great chelating candidates for the extraction of mercury. Thioureas have been selected to be used as functionalization in modified compounds for polymer matrices to recover heavy metals.[13,40] Various thiourea and sulfur-containing commercial and synthetic polymers have been described in the literature for the recovery of Hg[3,4,6,18,38,41–45] According to these studies, the covalent introduction of thiourea into the resin matrix is an attractive route for the preparation of chelating polymers with high capacity and selectivity for mercury removal.

To the best of our knowledge, no thiourea functionalized phenolic resins have been described for mercury removal from water. Herein, we present the synthesis of formo-phenolic resins with thiourea phenolic monomers obtained by a condensation polymerization for the removal of mercury. Adsorption kinetics, isotherm and thermodynamics models were investigated in order to better understand the adsorption mechanism of Hg (II) on the synthetic resins.

The selectivity of the resins towards other heavy metals and the desorption of the loaded material were also studied.

Results and Discussion

Resin synthesis and characterizations

The resin synthesis procedure was based on our previous work.[46] Resole type resins were prepared using an excess of formaldehyde compared to monomers in basic medium. The resin preparation is represented in Figure 1. The prepolymer was prepared by copolymerizing 1eq of thiourea monomer (C1, C2, C3, C4) or 1 eq of two monomers (0.5 eq of each monomer), (C1+C2, or C3+C4) with 2.5 eq of formaldehyde and 1.5 or 2 eq of base in water. In the presence of benzoyl and acetyl derivatives, DBU was used as an alkaline agent instead of NaOH to prevent the hydrolysis of the monomer that occurs in the presence of hydroxide. The progress of the prepolymerization was monitored by ^{1}H and ^{13}C DEPT 135 NMR spectroscopy allowing to follow the gradual formation of hydroxymethyl substituents (appearance of a CH_2 signal with a chemical shift at around 60 ppm). After 12 h at 60 °C, the reaction was stopped
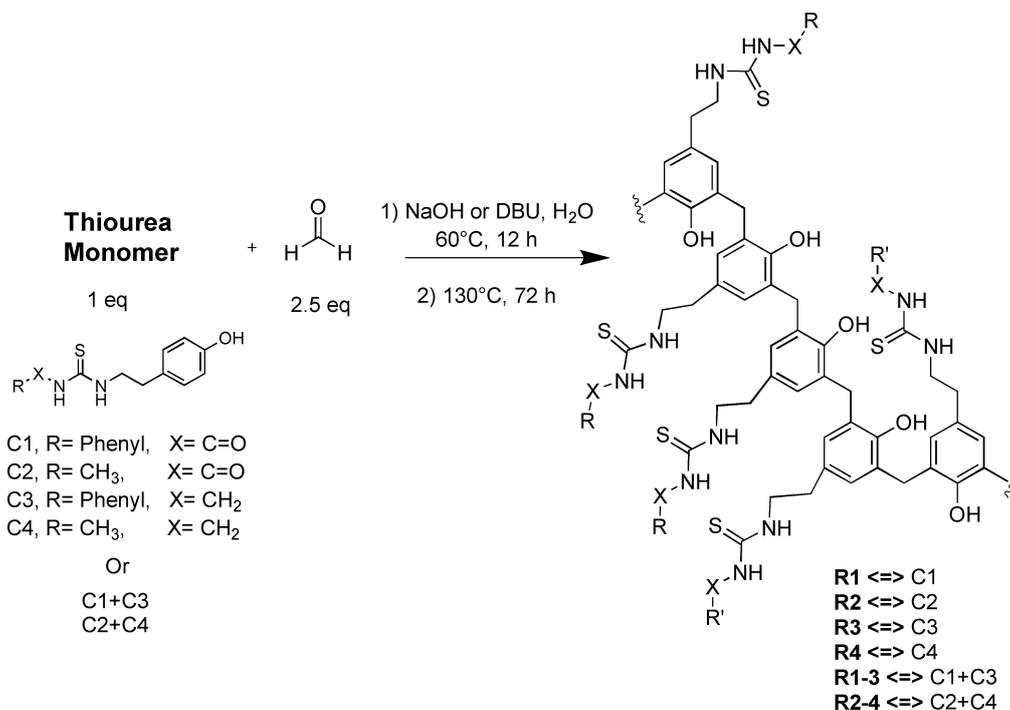
Figure 1. Synthesis scheme of the resins investigated for adsorption of Hg (II).

ChemistrySelect

Research Article
doi.org/10.1002/slct.202303015

**Chemistry
Europe**
European Chemical
Societies Publishing

and the prepolymer obtained was heated in an oven at 130 °C for 72 h.

The decrease in mass of the resins obtained after washing and conditioning, (H_2O, 1 mol/L HCl, H_2O) can be attributed to the removal of the additional reagent and partially soluble oligomeric species. Each resin was then ground in a ball mill (10 min, 25 Hz) to obtain a homogeneous particle size and surface contact. As a result, an insoluble, amorphous, infusible and cross-linked polymers were obtained (**R1**, **R2**, **R3**, **R4**, **R1-2** and **R3-4**). The IR spectra for the monomer and the resin highlight the presence of the thiourea precursor in the resin matrix. The complete characterization of the resins **R1**, **R2**, **R3**, and **R4** have been provided in a previous study.[46] The IR spectra of **R1-2**, and **R3-4** with their corresponding monomers are shown in Figure 2. The IR spectrum of the resins and their corresponding monomers were characterized by different bands well related to the phenolic monomer of thiourea.

The wide peaks at 3350 cm^{-1} are attributed to N—H and O—H stretched vibrations ($v_{(N-H)}$ and $v_{(O-H)}$), while the presence of thiourea is indicated by the prominent C=S stretched vibration ($v_{(C=S)}$) detected at about 1200 and 800 cm^{-1}. Furthermore, the absorption bands at about 1280 and 1500 cm^{-1}, corresponding to the N—C=S ($v_{(N-C=S)}$) and C—N fragments ($v_{(C-N)}$), respectively, provided additional evidence for the presence of thiourea. The structural characteristics were confirmed by the presence of the C=O stretching vibration band ($v_{(C=O)}$) at about 1670 cm^{-1}. These values are in agreement with the literature.[13,47,48]

The elemental composition of the various resins was evaluated giving the chemical composition of these materials and highlighting the presence of the sulfur in their matrix (Table S1).

The solid-state ^{13}C MAS NMR analyses of **R1-2**, and **R3-4** illustrated in Figure 3, show an aromatic carbon shift at 125 ppm, a phenolic carbon at 145 ppm, and a methylene bridge carbon at about 30 ppm, consistent with the other analysis.[46,49]

The thermal properties of the resins, thermal stability and moisture regain were determined by TGA measurement under air and nitrogen atmosphere. The TGA curves and their derivatives for the resins **R1-2**, and **R3-4** are shown in Figure S1. Endothermic peaks in the derivative thermogravimetric curves showed the thermal decomposition of the resins with three stages of decomposition for all polymers.

From 20 to 100 °C, the weight loss corresponds to the elimination of adsorbed water. From 200 to 400 °C, all resins showed the beginning of weight loss of the polymers. This second mass loss could be related to the oxidation of remaining methylols and methylene bridges and the degradation of other organic grafted moieties on the resins. The third weight loss from around 500 °C is related to the decomposition of the polymer matrix, yielding CO and CO_2, benzaldehyde, and char.[50–52]

Sorption Experiments

Equilibrium sorption isotherm

The sorption isotherm represents the distribution of the adsorbates between the solid (adsorbent) and liquid phases at equilibrium. It is based on the relationship between two
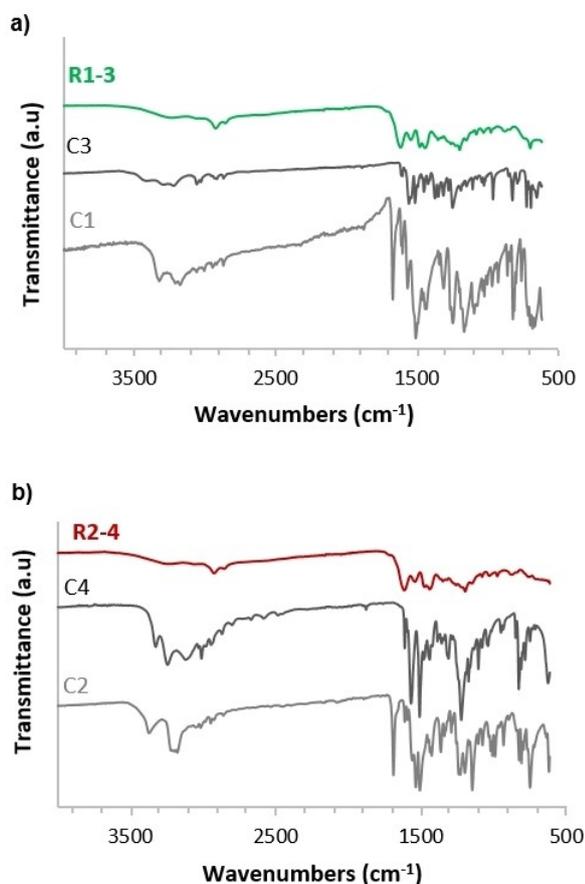
Figure 2. FTIR spectra for a) **R1-3**, and b) **R2-4** polymer and their respective thiourea ligand.
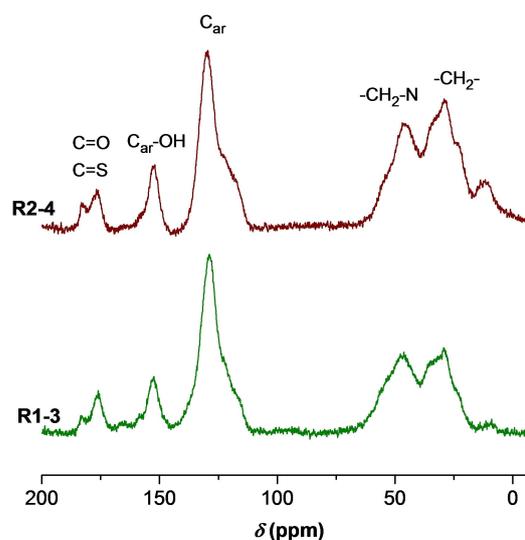
Figure 3. ^{13}C solid-state NMR spectra of **R1-3**, and **R2-4**

parameters, the adsorption capacity (Q_e) and the equilibrium metal ion concentration (C_e) in the liquid phase at constant temperature and pH.

The sorption experiment was carried out at 25 °C and pH<7 in order to avoid the precipitation of the metal ions. The effect of pH on the extraction of Hg was investigated. The results showed that there was no effect on the extraction for pH ranging from 1 and 5 (Figure S2). The extraction capacity and selectivity of the mercury through **R1**, **R2**, **R3**, **R4**, **R1-2** and **R3-4** were investigated. The experiments were performed by contacting 10 mg of resin with 10 mL of metal solution. The initial concentration of metals was varied from 20 to 500 mg/L, while the other parameters (pH, T °C, rpm) were kept constant.

For **R1**, **R3**, **R1-2**, and **R3-4**, the results showed that they have a good affinity for the removal of mercury, as represented in Figure 4(a). The extraction showed a rapid increase at low concentrations, then, a plateau was reached for the higher values. However, for **R2** and **R4** resins based on C2 and C4 respectively, the results showed that they did not exhibit a significant affinity for mercury recovery (Figure S3).

Langmuir and Freundlich isotherms were used to describe the sorption of Hg (II) on **R1**, **R2**, **R1-2**, and **R3-4** resins. By comparing the fitting isotherms for the two models (Figure 4(b) and Figure S4), the Langmuir isotherm was found to be the most suitable model to describe the adsorption of mercury on the different resins with a high correlation coefficient R^2, while the Freundlich isotherms showed a non-linear fit. The Langmuir model assumes a homogeneous adsorbent surface, no interaction between adsorbed species (they behave independently), and a monolayer adsorption process.[53]

Based on the Langmuir isotherm, the maximum loading capacity of the resin (Q_{max}) was determined from the slopes and the intercepts of the plots (Figure 4(b)). As a result, the Q_{max} values for **R1**, **R3**, **R1-2**, and **R3-4** for Hg were estimated to be 78, 150, 310, and 295 mg/g, respectively. There was a difference in the affinity between **R1** and **R3** which are based on the benzoyl and acetyl thiourea monomers respectively. This resulted in a twofold increase in extraction capacity. This could be related to the steric hindrance of the binding site environment that is provided by the presence of phenyl. For **R1-2** and **R3-4** that are based on the presence of two different thiourea monomers, a similar affinity for the recovery of Hg was obtained, but with a higher capacity than those of **R1** and **R3**. In general, by comparison with **R2** and **R4**, it could be suggested that the presence of C=O plays a significant role in the chelation of mercury. However, at high concentrations, at 100 % of the monomers C1 and C2, there was a probability that hydrogen bonding will occur in the reticulation steps, limiting mercury from easy access to the chelation sites. This is confirmed by the fact that the addition of a co-monomer in the case of **R1-2** and **R3-4** leads to a dilution of the matrix, making the sites more accesible, resulting in a doubling of the extraction capacity.

Based on the rapid increase at low concentrations, it was concluded that the resins have a high affinity for Hg (II) metals. In terms of adsorption energy, it can be assumed that the surface of the adsorbent is uniform, homogeneous, and all sites are energetically equivalent for the chelation of Hg by these resins. Mercury chelation responds well to HSAB theory, and it has been shown to be influenced by the binding site environment. Examination of the resins by SEM, showed smooth glass-like surface particles and confirm the presence of the functional group and mercury in the polymer after the sorption experiments (Figure S5 and S6).

Kinetic studies

The adsorption kinetics of Hg using the four resins, are shown in Figure 5. Adsorption kinetics provide information about the rate of adsorption and the time required to reach equilibrium. The kinetic adsorption of Hg (II) on the resins was evaluated at room temperature and pH 4 (Figure 5(a)). The kinetic experi-

Figure 4. a) Adsorption isotherms yielded for Hg on **R1**, **R3**, **R1-2**, and **R3-4**; b) Plot of Langmuir isotherm equation for Hg adsorption by **R1** ($y = 0.0128x + 0.0207$ $R^2 = 0.9950$), **R3** ($y = 0.0067x + 0.0113$ $R^2 = 0.9987$), **R1-2** ($y = 0.0032x + 0.007$ $R^2 = 0.9995$), and **R3-4** resins ($y = 0.0034x + 0.0058$ $R^2 = 0.9987$). Extraction experiments: 10 mL of Hg (20 to 500 mg/L of elements at pH = 4), contacted with 10 mg of resin **R1**, **R3**, **R1-2**, and **R3-4** for 24 h at 25 °C.

ChemistrySelect

Research Article
doi.org/10.1002/slct.202303015

Chemistry Europe
European Chemical
Societies Publishing
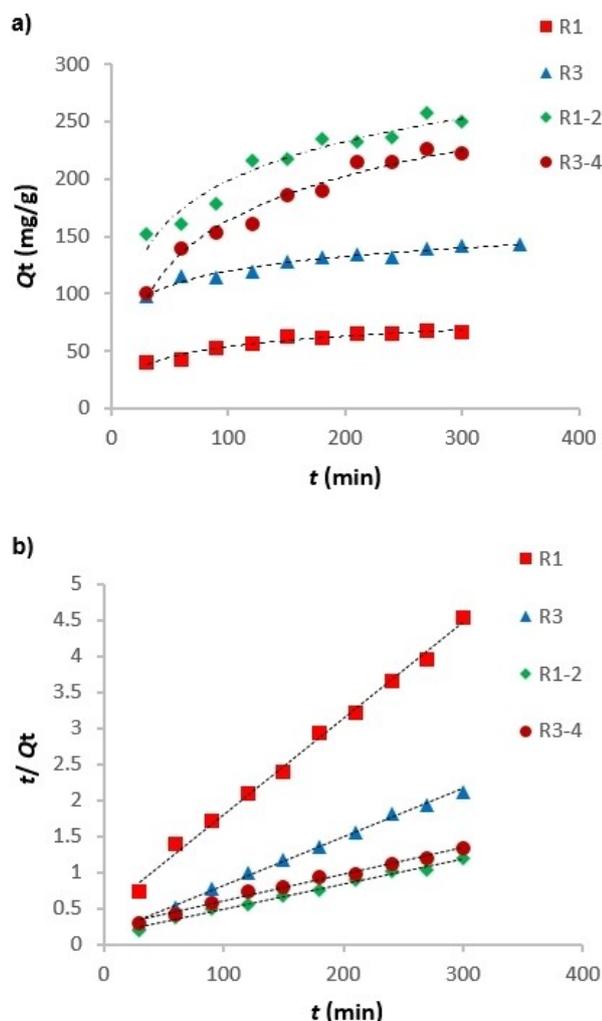
Figure 5. Adsorption Kinetics studies of Hg by **R1**, **R3**, **R1-2**, and **R3-4**. a) kinetic adsorption isotherm, **R1** ($y = 13.201 \ln(x) - 6.8026$ $R^2 = 0.9558$), **R2** ($y = 18.298 \ln(x) + 35.637$ $R^2 = 0.9645$), **R1-2** ($y = 55.71 \ln(x) - 92.608$ $R^2 = 0.973$), and **R3-4** resins ($y = 49.159 \ln(x) - 27.737$ $R^2 = 0.9337$). b) pseudo second order fitted isotherm **R1** ($y = 0.0133x + 0.4824$ $R^2 = 0.9955$), **R3** ($y = 0.0067x + 0.1505$ $R^2 = 0.9964$), **R1-2** ($y = 0.0035x + 0.1451$ $R^2 = 0.9904$), and **R3-4** resins ($y = 0.0037x + 0.2339$ $R^2 = 0.9875$). Extraction experiments: 10 mL of Hg (200 mg/L) at pH = 4 contacted with 10 mg of resin **R1** for 0–5 h at 25 °C; 10 mL of Hg (300 mg/L) at pH = 4 contacted with 10 mg of resin **R3**, **R1-2**, and **R3-4** for 0–5 h at 25 °C.

ment indicates that the adsorption of Hg reached a plateau and therefore the equilibrium was about 5 h for the four resins.

In order to evaluate and understand the process dynamics and predict the adsorption state over time, the adsorption kinetic data were fitted with pseudo-first-order (Figure S7) and pseudo-second-order (Figure 5(b)) kinetic models as discussed in the experimental section. The adsorption behavior of mercury per unit time follows the pseudo-second order model. In fact, the correlation coefficient of the adsorption kinetics of mercury using the pseudo-second-order model is higher than that of the pseudo-first-order model (Table 1). In addition, the calculated Q_e values of this model are closer to the value obtained from the adsorption isotherm.

Therefore, the results clearly showed that the pseudo-second order model was more suitable to describe the adsorption kinetic processes of different resins for Hg (II). This indicates that the adsorption rate depends on the adsorption capacity and not on the concentration of adsorbates as defined by the chemical sorption, or chemisorption phenomenon.[54,55]

Influence of Temperature

Adsorption experiments at different temperatures were performed to determine the influence of the temperature on the adsorption capacity. The adsorption isotherms of **R1**, **R3**, **R1-2**, and **R3-4** towards Hg (II) at different temperatures are shown in Figure 6.

In general, it can be seen that the adsorption capacities increase with the increase of the temperature, indicating that the adsorption occurs by a chemical process. Between 15 and 25 °C, **R1** and **R3** resins do not show any significant change in the adsorption process, but when the temperature was increased to 35 °C, a significant modification occurred. The adsorption capacities of the resins towards Hg increased from 78 to 120 mg/g for **R1** and from 150 to 250 mg/g for **R3**. However, a different mechanism was observed for **R1-2** and **R3-4** than for the other two resins. The adsorption capacity of the resins increased significantly between 15 and 25 °C for both resins in the order of 100 mg/g, while a very slight change was observed between 25 and 35 °C. Therefore, the resins do not exhibit the same adsorption process for the recovery of Hg. For

Table 1. Kinetic parameters for Hg (II) uptake on **R1**, **R2**, **R1-3**, and **R2-4**.

Kinetic Model	Resins	Q_e (mg.g^{-1})	k_1 (min^{-1})	k_2 (g.mg^{-1}.min^{-1})	R^2
Pseudo-First Order	R1	40.51	4.836×10^{-3}		0.921
	R2	58.64	6.218×10^{-3}		0.951
	R1-3	159.11	5.527×10^{-3}		0.927
	R2-4	189.06	4.606×10^{-3}		0.961
Pseudo-Second Order	R1	75.18		3.667×10^{-4}	0.995
	R2	149.25		2.983×10^{-4}	0.996
	R1-3	285.71		8.443×10^{-5}	0.990
	R2-4	270.27		5.853×10^{-5}	0.987

ChemistrySelect

Research Article
doi.org/10.1002/slct.202303015

Chemistry Europe
European Chemical
Societies Publishing
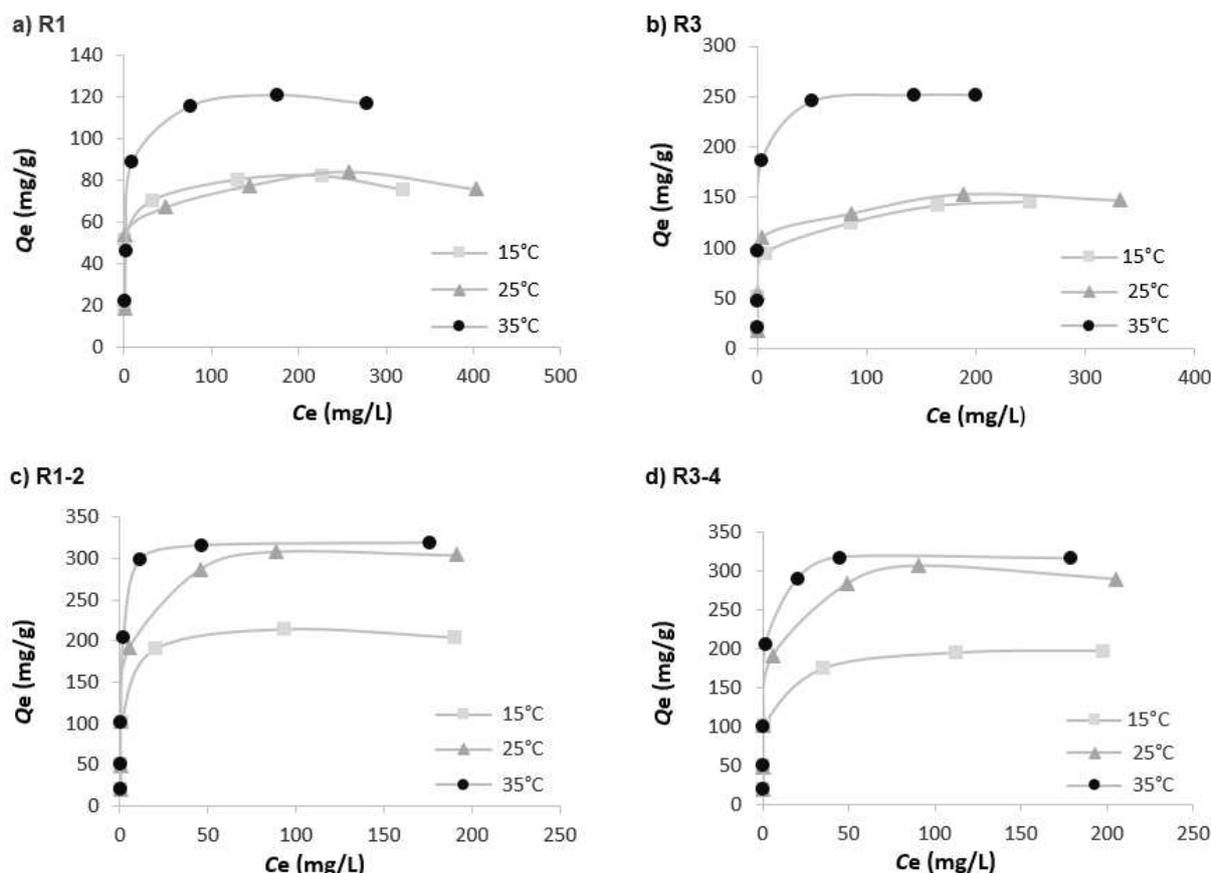
Figure 6. Adsorption isotherms yielded for Hg: a) **R1**, b) **R3**, c) **R1-2**, d) **R3-4** at different temperature; Extraction experiments: 10 mL of Hg (20 to 500 mg/L at pH = 4), contacted with 10 mg of resin **R1**, **R2**, **R1-2**, and **R3-4** for 24 h at 15, 25, and 35 °C.

R2 and **R4**, there is no change in affinity even when the temperature was increased to 35 °C (Figure S3).

Thermodynamic studies

For all resins, except **R3**, it was impossible to determine the thermodynamic parameters such as Gibbs (ΔG^0), enthalpy (ΔH^0), and entropy (ΔS^0) of the adsorption, because the original order of the Langmuir adsorption fit isotherm was too close to zero. This made the data recovery difficult.

For **R3**, the thermodynamic parameters were calculated from the slope and the intercept of the Van't Hoff equations as represented in the experimental section. The fitted Van't Hoff equations for different resins are shown in Figure S8, and the obtained parameters for **R3** are given in the Table S2. The positive value of ΔH for **R3** indicated that the adsorption of Hg (II) into this resin was endothermic, and the negative value of ΔG showed that the adsorption process was spontaneous.[13]

Selectivity

An experiment was carried out to investigate the selectivity of the resins towards mercury compared to other heavy metals

(Pb, Cd, Zn, Ni, and Cu). Figure 7(a) shows that the resins have higher selectivity for Hg (II) than for Pb (II) and Cd (II). According to the HSAB theory, soft elements have a high affinity for soft bases with O < N < S donor atoms. This explains the affinity of these thiourea-based resins for the soft acid Hg. For Pb, the non-affinity can be explained by the fact that it is classified as an intermediate element, neither very soft nor very hard.

Although Cd is well classified as a soft acid, the resin could not show any affinity for the Cd recovery. The loss of affinity can be explained by the other variables that can potentially affect the adsorption of a metal, such as the degree of oxidation and the environment of the binding site (steric bulk…). In addition, these resins exhibit high selectivity for Hg recovery compared to Cu, Zn and Ni (Figure 7(b)). These results are well correlated with Pearson's theory because these elements are considered as hard acid or intermediate. The S factor of the selectivity for Hg compared to the other listed elements is higher than 500.

Desorption

In order to regenerate the Hg (II) loaded sorbent, different solutions of the loaded adsorbent were used. The use of thiourea solution at different concentrations and pH values
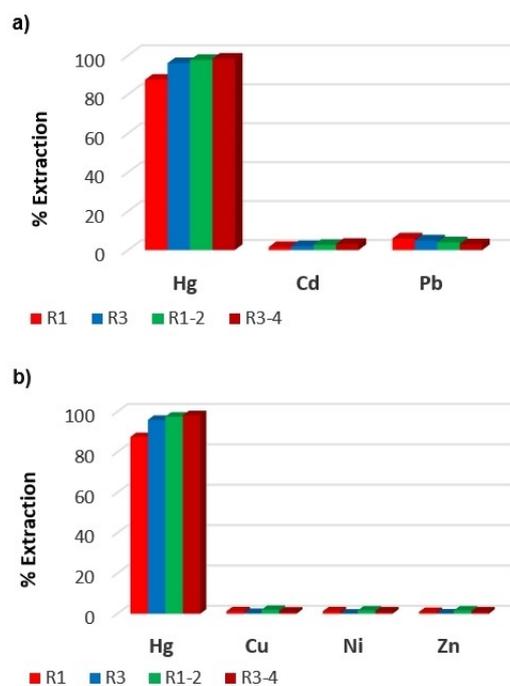
Figure 7. Selective extraction experiment: a) 10 mL of a mixture of Hg, Cd, and Pb 100 mg/Lof each elements at pH = 4 contacted with 10 mg of resin **R1**, **R3**, **R1-2** or **R3-4** for 24 h at 25 °C; b) 10 mL of a mixture of Hg, Cu, Ni, and Zn 100 mg/L of each elements at pH = 4 contacted with 10 mg of resin **R1**, **R3**, **R1-2** or **R3-4** for 24 h at 25 °C.

resulted in successful desorption. The efficiency of the desorption process was highlighted by comparing the EDX spectra before and after the desorption of Hg (II), with the absence of peaks corresponding to Hg after the desorption process (Figure S9).

The adsorption-desorption cycles were performed three times using a solution of 100 mg/L Hg (II) metal ions and 1 M thiourea at pH 2 as the desorption solution. The determined desorption capacities after multiple regenerations are shown in Table 2. These results demonstrate the reusability of polymeric adsorbents without loss of capacity. Therefore, due to their high efficiency and recyclability, these thiourea-formophenolic resins are suitable adsorbents for Hg (II) recovery.

Comparison with further sorbents

Adsorption efficiency depends on a variety of factors, including the type of adsorbent, its functionalization, and the experimental parameters involved in the adsorption experiment, such as metal ion concentration, solid/liquid ratio, pH, ionic strength, and temperature. Therefore, it is difficult to evaluate different sorbents in a relevant way. As an indication, the Q_{max} values for Hg (II) removal for different sorbents functionalized with sulfur moieties are given in Table 3, and compared to the literature,[56–60] competitive maximum adsorption capacities were obtained in this work.

Conclusions

New chelating sorbents based on phenolic thiourea monomers were obtained by alkaline condensation polymerization reaction. The resins were used for the recovery of mercury by adsorption process. They showed a good affinity for mercury and it was not affected by pH values between 1 and 5. The extraction capacities for resins **R1**, **R3**, **R1-2**, and **R3-4** towards Hg are 78 mg/g, 150 mg/g, 310 mg/g, and 295 mg/g respectively.

These resins also showed higher selectivity for Hg (II) compared to other heavy metals: Pb (II), Cd (II), Zn (II), Cu (II) and Ni (II).

The isothermal adsorption study for the different resins showed that the adsorption was a Langmuir monolayer process exhibiting chemisorption process. These results were confirmed by the kinetic studies, which followed a pseudo-second order.

Table 2. Hg sorption and desorption efficiencies for R1.

	Hg sorption (%)	Hg recovery (%)
Cycle 1	99.97	98.77
Cycle 2	99.89	98.58
Cycle 3	99.06	97.99

Sorption experiments: 10 mL of Hg solution at 100 mg/L, pH = 4, contacted with 10 mg of resin R1 for 24 h at 25 °C; Desorption experiments: 10 mL of 1 mol/L thiourea solution, pH = 2, contacted with 10 mg of resin loaded R1-Hg for 24 h at 25 °C.

Table 3. Comparison of sorbent for Hg (II) removal.

Sorbent	Q_{max} (mg/g)	Experimental condition	Reference
Thiourea-phenolic resins	285	[Hg (II)] = 300 mg/L; pH = 4; S/L = 1 (10/10); 5 h at 25 °C	This study
Thioacetamide/chitosan	195	[Hg (II)] = 200 mg/L; pH = 5; S/L = 1 (50/50); 2 h at 25 °C	[56]
Poly(2-aminothiophenol)/biochar	286	[Hg (II)] = 100 mg/L; pH = 7; S/L = 0.75 (750/1000); 5 h at 25 °C	[57]
Thiol/ Zr- MOF (Zr-DMBD)	171	[Hg (II)] = 300 mg/L; pH = 6; S/L = 1 (20/20) 10 min at 25 °C	[58]
Dithiocarbamate/silica ge	115	[Hg (II)] = 180 mg/L; pH = 4; S/L = 1 (20/20); 10 h at 25 °C	[59]
Thiol/poly(glycidyl methacrylate)	51	[Hg (II)] = 300 mg/L; pH = 7; S/L = 2 (100/50); 4 h at 25 °C	[60]

S/L: Solid/Liquid ratio (S (mg) / L (mL))

The thermodynamic study showed that the extraction process is spontaneous and endothermic.

Based on these different results, these polymeric materials can be considered as promising sorbents for the removal of mercury from aqueous effluents. Preliminary studies indicated that Hg could be removed from the loaded resins using a 1 mol/L thiourea desorption solution at pH = 2 and reused without any treatment. Further work should include the implementation of continuous sorption using these resins in column form.

Experimental Section

Materials and methods

All chemicals and solvents were analytically pure from Sigma Aldrich, France and were used without further purification. The heavy metal solutions were prepared from the ICP standard (in 1% HNO_3 or HCl from ICP Science, 10 g/L).

General procedure for resins synthesis

With respect to our previous work,[46] substituted thiourea monomers were synthesized via a known synthetic route in two steps, similar to the procedure reported in literature.[47] The resins were also synthesized via alkaline polycondensation of an aldehyde, formaldehyde, with phenolic compounds according to the literature procedures.[49,61–63]

The thiourea phenolic precursors were introduced into a double-necked round-bottom flask equipped with a condenser and a magnetic stirrer. It was dissolved in an alkaline solution using 1.5 eq of sodium hydroxide or 2 eq of 1,8-diazabicyclo(5.4.0)undec-7-ene (DBU) and 80 eq of water. After complete dissolution of the phenolic compound, formaldehyde (2.5 eq) was added and the mixture was stirred for 24 h at 60 °C. The reaction mixture was analyzed periodically by ^1H and ^{13}C DEPT 135 NMR to follow the progress of the prepolymerization. The resulting prepolymer was then heated in an oven in air at 130 °C for 72 h. After curing, the polymer was ground by a ball mill and washed with H_2O, 1 mol/L HCl to remove unreacted compounds and the uncrosslinked oligomers. The resin was then dried at 80 °C overnight.

Resin Characterization Techniques

Fourier Transform Infrared (FTIR) spectroscopy analysis was performed on a Perkin Elmer 100 spectrometer between 615 and 4000 cm^{-1} using an ATR crystal with resolution of 4 cm^{-1}. An elemental analyzer (Elementar Vario Micro Cube Instrument) was used to determine the chemical composition of the resins.

A Scanning Electron Microscopy (SEM) was performed using a Quattro S Environmental Scanning Electron Microscope (Thermo-Fisher) instrument in order to study and observe the morphology of the resins. Microscale observations were coupled with an EDX elemental probe (XFlash6 / 100), which allowed semi-quantitative chemical analysis of areas of interest. Thermogravimetric Analysis (TGA) was carried out with a Mettler Toledo equipment under air or nitrogen flow at a heating rate of 10 °C/min from 25 to 950 °C. To determine the moisture regain of the resins, an additional isothermal treatment at 100 °C for 30 minutes was performed under air. The resins were mechanically crushed using a Retsch mixer mill MM 200 and a Zr ball for 10 minutes at 25 Hz.

^1H and ^{13}C NMR spectra were carried out in DMSO as a deuterated solvent using a Bruker Advance 400 MHz instrument in order to follow the progress of the reactions.

The ^{13}C Solid-state MAS NMR spectra were recorded at rotation speed of 12 KHz (4 mm outer diameter rotors) using a Bruker Advance 400 MHz.

Metal concentrations were determined before and after the extraction using an Inductively Coupled Plasma/Atomic Emission Spectroscopy (ICP/OES ICAP Pro spectrometer from Thermo Scientific). The wavelengths used for the measurements were chosen to avoid spectral interference between the elements analyzed.

Sorption experiments

The solutions of the heavy metals, Mercury (Hg^{2+}), Lead (Pb^{2+}) and Cadmium (Cd^{2+}) were prepared from a 10 g/L ICP standard (in 1% HCl from ICP Science) after dilution with deionized water. The solutions of Zinc (Zn^{2+}), Copper (Cu^{2+}), and Nickel (Ni^{2+}) were prepared from their chlorate salts. Sorption experiments were carried out in batch systems using 10 mg of resin equilibrated with 10 mL of metal solutions. To ensure equilibrium, batch contacts were typically run for 24 hours. Samples were collected and filtered through a 0.2-micron cellulose filter. The filtrates were then analyzed by ICP/OES after dilution (1% HNO_3, and 1% HCl) to determine the amount of residual metals ion.

Typically, the following procedure was used: 10 mL of Hg (20 to 500 mg/L of elements at pH = 4), contacted with 10 mg of resin **R1**, **R3**, **R1-2**, and **R3-4** for 24 h at 15, 25 or 35 °C. For the selectivity experiment 10 mL of a mixture of Hg, Cu, Ni, and Zn at 100 mg/L of each elements at pH = 4 was contacted with 10 mg of resin **R1**, **R3**, **R1-2** or **R3-4** for 24 h at 25 °C.

The adsorption efficiency E (%), the adsorption capacity Q_e (mg/g) and the selectivity $(S_{A/B})$ were calculated as reported in our previous work.

For the sorption isotherm, the equilibrium of adsorption has been described using Langmuir, and Freundlich isotherms.[64,65] These two models are represented by Eq. 1 and Eq. 2, respectively. Where, C_e (mg/L) and Q_e (mg/g) are the equilibrium metal ion concentrations in the liquid phase and in the solid phase respectively, Q_{max} (mg/g) is the maximum metal ion adsorbed per unit mass of adsorbent, and K (L/mg) is the Langmuir or Freundlich constant.

$$\frac{C_e}{Q_e} = \frac{1}{Qmax} \times C_e + \frac{1}{K \times Qmax} \tag{1}$$

$$InQ_e = InK + \frac{1}{n}InC_e \tag{2}$$

Adsorption kinetic

For uptake kinetics, the experiment was conducted in the same manner as for batch contacts, except that aliquots of the supernatant were analyzed periodically by ICP/OES.

Typically, the following procedure was used: 10 mL of Hg (300 mg/L) at pH = 4 contacted with 10 mg of resin **R3**, **R1-2**, and **R3-4** for 0–5 h at 25 °C.

ChemistrySelect

Research Article
doi.org/10.1002/slct.202303015

Chemistry Europe
European Chemical
Societies Publishing

The kinetic data were fitted using pseudo first- and second order-kinetic models.[66–68] These two models are defined in Eq. 3 and Eq. 4, respectively.

$$\log(Q_e - Q_t) = \log Q_e - \frac{k_1}{2.303} \times t \qquad (3)$$

$$\frac{t}{Q_t} = \frac{1}{Q_e} \times t + \frac{1}{k_2 \times Q_e^2} \qquad (4)$$

Where Q_e (mg/g) and Q_t (mg/g) are the equilibrium metal concentration in the solid phase and in the solid phase at time t, respectively, k_1 (min^{-1}) and k_2 (g.mg^{-1}.min^{-1}) are the pseudo first-order and second order equilibrium rate constant, respectively.

Thermodynamic Studies

Thermodynamic parameters are essential to better understand how the temperature affects the adsorption process and to determine whether the process is spontaneous. These parameters include the change in enthalpy ($\Delta H°$), entropy ($\Delta S°$) and Gibbs free energy ($\Delta G°$). They were estimated from the slope and intercept of the Van't Hoff equations as shown in Eq. 5 and Eq. 6. Where, K_L (mL.mmol^{-1}) is the Langmuir constant, R (J.mol^{-1}.K^{-1}) is the gas constant, and T (K) is the temperature.[64,69,70]

$$\ln K_L = \frac{\Delta S}{R} - \frac{\Delta H}{RT} \qquad (5)$$

$$\Delta G = \Delta H - T\Delta S \qquad (6)$$

Supporting Information

The following supporting information are available:

Figure S1: Thermogravimetric analysis for **R1-2** and **R3-4**

Figure S2: pH extraction experiments

Figure S3: Adsorption isotherm for **R2** and **R4**

Figure S4: Plot of Freundlich isotherm equation

Figure S5: SEM images of **R3**

Figure S6: SEM-EDX cartography for **R3** loaded with Hg

Figure S7: Adsorption Kinetics studies

Figure S8: Thermodynamic studies

Figure S9: Pre and post desorption EDX analysis

Table S1: Elemental analysis

Table S2: Thermodynamic parameters for sorption with **R3**

Conflict of Interests

The authors declare no conflict of interest.

Data Availability Statement

The data that support the findings of this study are available from the corresponding author upon reasonable request.

[1] F. Fu, Q. Wang, *J. Environ. Manage.* **2011**, *92*, 407–418.
[2] Y. Zhang, X. Ji, T. Ku, G. Li, N. Sang, *Environ. Pollut.* **2016**, *216*, 380–390.
[3] T. Velempini, K. Pillay, *J. Environ. Chem. Eng.* **2019**, *7*, 103350.
[4] W. Zhuo, H. Xu, R. Huang, J. Zhou, Z. Tong, H. Xie, X. Zhang, *J. Iran. Chem. Soc.* **2017**, *14*, 2557–2566.
[5] J. D. Merrifield, W. G. Davids, J. D. MacRae, A. Amirbahman, *Water Res.* **2004**, *38*, 3132–3138.
[6] F.-Q. An, Y. Wang, X.-Y. Xue, T.-P. Hu, J.-F. Gao, B.-J. Gao, *Chem. Eng. Res. Des.* **2018**, *130*, 78–86.
[7] S. Lata, P. K. Singh, S. R. Samadder, *Int. J. Environ. Sci. Technol.* **2015**, *12*, 1461–1478.
[8] *Directive 2008/105/EC – Environmental Quality Standards in the Field of Water Policy, Amending and Subsequently*, The European Parliament, **2008**.
[9] *Guidelines for Drinking-Water Quality: Fourth Edition Incorporating the First and Second Addenda.*, World Health Organization, Geneva, **2022**.
[10] M. Kumar, A. Puri, *Indian J. Occup. Environ. Med.* **2012**, *16*, 40–44.
[11] C.-C. Lin, N. Yee, T. Barkay, in *Environmental Chemistry and Toxicology of Mercury*, John Wiley & Sons, Ltd, **2011**, pp. 155–191.
[12] A. R. Kadam, G. B. Nair, S. J. Dhoble, *J. Environ. Chem. Eng.* **2019**, *7*, 103279.
[13] X. Yao, H. Wang, Z. Ma, M. Liu, X. Zhao, D. Jia, *Chin. J. Chem. Eng.* **2016**, *24*, 1344–1352.
[14] C. Namasivayam, K. Kadirvelu, *Carbon* **1999**, *37*, 79–84.
[15] D. Martín-Yerga, M. B. González-García, A. Costa-García, *Talanta* **2013**, *116*, 1091–1104.
[16] R. Chakraborty, A. Asthana, A. K. Singh, B. Jain, A. B. H. Susan, *Int. J. Environ. Anal. Chem.* **2022**, *102*, 342–379.
[17] G. Zuo, M. Muhammed, *React. Funct. Polym.* **1995**, *27*, 187–198.
[18] A. M. Donia, A. A. Atia, A. M. Heniesh, *Sep. Purif. Technol.* **2008**, *60*, 46–53.
[19] A. Azimi, A. Azari, M. Rezakazemi, M. Ansarpour, *ChemBioEng Rev.* **2017**, *4*, 37–59.
[20] V. Gunarathne, A. U. Rajapaksha, M. Vithanage, D. S. Alessi, R. Selvasembian, Mu. Naushad, S. You, P. Oleszczuk, Y. S. Ok, *Crit. Rev. Environ. Sci. Technol.* **2022**, *52*, 1022–1062.
[21] J. F. Blais, Z. Djedidi, R. B. Cheikh, R. D. Tyagi, G. Mercier, *Pract. Period. Hazard. Toxic Radioact. Waste Manag* **2008**, *12*, 135–149.
[22] A. Da̧browski, Z. Hubicki, P. Podkościelny, E. Robens, *Chemosphere* **2004**, *56*, 91–106.
[23] N. M. Bandaru, N. Reta, H. Dalal, A. V. Ellis, J. Shapter, N. H. Voelcker, *J. Hazard. Mater.* **2013**, *261*, 534–541.
[24] M. Zaib, M. M. Athar, A. Saeed, U. Farooq, *Biosens. Bioelectron.* **2015**, *74*, 895–908.

[25] M. Xia, Z. Chen, Y. Li, C. Li, N. M. Ahmad, W. A. Cheema, S. Zhu, *RSC Adv.* **2019**, *9*, 20941–20953.

[26] P. Hadi, M.-H. To, C.-W. Hui, C. S. K. Lin, G. McKay, *Water Res.* **2015**, *73*, 37–55.

[27] B. Zeng, G. Lin, J. Li, W. Wang, L. Zhang, *Process Saf. Environ. Prot.* **2022**, *168*, 123–132.

[28] L. Wang, D. Hou, Y. Cao, Y. S. Ok, F. M. G. Tack, J. Rinklebe, D. O'Connor, *Environ. Int.* **2020**, *134*, 105281.

[29] S. S. Ghasemi, M. Hadavifar, B. Maleki, E. Mohammadnia, *J. Water Proc. Eng.* **2019**, *32*, 100965.

[30] J. Jiang, X.-S. Ma, L.-Y. Xu, L.-H. Wang, G.-Y. Liu, Q.-F. Xu, J.-M. Lu, Y. Zhang, *e-Polym.* **2015**, *15*, 161–167.

[31] U. U. Jadhav, H. Hocheng, *J. Achiev. Mater. Manuf. Eng.* **2012**, *54*, 159–167.

[32] P. Lu, T. Chen, H. Liu, P. Li, S. Peng, Y. Yang, *Minerals* **2019**, *9*, 74.

[33] H. Chen, Y. Gao, J. Li, Z. Fang, N. Bolan, A. Bhatnagar, B. Gao, D. Hou, S. Wang, H. Song, X. Yang, S. M. Shaheen, J. Meng, W. Chen, J. Rinklebe, H. Wang, *Carbon Research* **2022**, *1*, 4.

[34] S. Chu, X. Feng, C. Liu, H. Wu, X. Liu, *Ind. Eng. Chem. Res.* **2022**, *61*, 11309–11328.

[35] A. Lezzi, S. Cobianco, A. Roggero, *J. Polym. Sci. Part A* **1994**, *32*, 1877–1883.

[36] V. Camel, *Spectrochim. Acta Part B* **2003**, *58*, 1177–1233.

[37] R. S. Azarudeen, R. Subha, D. Jeyakumar, A. R. Burkanudeen, *Sep. Purif. Technol.* **2013**, *116*, 366–377.

[38] R. A. Silva, K. Hawboldt, Y. Zhang, *Miner. Process. Extr. Metall. Rev.* **2018**, *39*, 395–413.

[39] R. G. Pearson, *J. Am. Chem. Soc.* **1963**, *85*, 3533–3539.

[40] L. Wang, R. Xing, S. Liu, Y. Qin, K. Li, H. Yu, R. Li, P. Li, *Carbohydr. Polym.* **2010**, *81*, 305–310.

[41] N. Li, H. Wei, Y. Duan, H. Tang, S. Zhao, P. Hu, S. Ren, *Energy Fuels* **2018**, *32*, 11023–11029.

[42] M. Fayazi, *Environ. Sci. Pollut. Res. Int.* **2020**, *27*, 12270–12279.

[43] A. Lezzi, S. Cobianco, *J. Appl. Polym. Sci.* **1994**, *54*, 889–897.

[44] C. Ni, C. Yi, Z. Feng, *J. Appl. Polym. Sci.* **2001**, *82*, 3127–3132.

[45] L. Wang, R. Xing, S. Liu, S. Cai, H. Yu, J. Feng, R. Li, P. Li, *Int. J. Biol. Macromol.* **2010**, *46*, 524–528.

[46] C. El Khoueiry, F. Giusti, E. Lelong, G. Arrachart, B. Nsouli, I. Karame, S. Pellet-Rostaing, *Hydrometallurgy* **2024**, *223*, 106201.

[47] A. M. Alkherraz, Z. I. Lusta, A. E. Zubi, *Int. J. Environ. Anal. Chem.* **2014**, *8*, 108–110.

[48] C. Y. Panicker, H. Varghese, G. Abraham, P. Thomas, *Eur. J. Chem.* **2010**, *1*, 173–178.

[49] G. Arrachart, A. Kenaan, S. Gracia, R. Turgis, V. Dubois, S. Pellet-Rostaing, *Sep. Sci. Technol.* **2015**, *50*, 1882–1889.

[50] C. Arrambide, G. Arrachart, S. Berthalon, M. Wehbie, S. Pellet-Rostaing, *React. Funct. Polym.* **2019**, *142*, 147–158.

[51] W. M. Jackson, R. T. Conley, *J. Appl. Polym. Sci.* **1964**, *8*, 2163–2193.

[52] H. Jiang, J. Wang, S. Wu, Z. Yuan, Z. Hu, R. Wu, Q. Liu, *Polym. Degrad. Stab.* **2012**, *97*, 1527–1533.

[53] T. R. Sahoo, B. Prelot, in *Nanomaterials for the Detection and Removal of Wastewater Pollutants* (Eds.: B. Bonelli, F. S. Freyria, I. Rossetti, R. Sethi), Elsevier, **2020**, pp. 161–222.

[54] V. Vadivelan, K. V. Kumar, *J. Colloid Interface Sci.* **2005**, *286*, 90–100.

[55] B. Liu, H. Luo, H. Rong, X. Zeng, K. Wu, Z. Chen, H. Lu, D. Xu, *Desalin. Water Treat.* **2019**, *160*, 260–267.

[56] M. E. Eissa, A. K. Sakr, M. Y. Hanfi, M. I. Sayyed, J. S. Al-Otaibi, A. M. Abdel-lateef, M. F. Cheira, H. A. Abdelmonem, *Chemosphere* **2023**, *341*, 140062.

[57] M. S. Nejad, H. Sheibani, *J. Environ. Chem. Eng.* **2022**, *10*, 107363.

[58] L. Ding, X. Luo, P. Shao, J. Yang, D. Sun, *ACS Sustainable Chem. Eng.* **2018**, *6*, 8494–8502.

[59] J. Lu, X. Wu, Y. Li, W. Cui, Y. Liang, *Surf. Interfaces* **2018**, *12*, 108–115.

[60] H. H. Kim, T. G. Lee, *J. Ind. Eng. Chem.* **2017**, *47*, 446–450.

[61] C. Arrambide, S. Marie, G. Arrachart, S. Pellet-Rostaing, *Sep. Purif. Technol.* **2018**, *193*, 214–219.

[62] R. Oye Auke, G. Arrachart, R. Tavernier, G. David, S. Pellet-Rostaing, *Polymer* **2022**, *14*, 311.

[63] F. Bekkar, C. Arrambide, C. El Khoueiry, R. Meghabar, G. Arrachart, S. Pellet-Rostaing, *Mater. Res. Innovations* **2023**, *27*, 1–4.

[64] P. S. Ghosal, A. K. Gupta, *J. Mol. Liq.* **2017**, *225*, 137–146.

[65] G. Limousin, J.-P. Gaudet, L. Charlet, S. Szenknect, V. Barthès, M. Krimissa, *Appl. Geochem.* **2007**, *22*, 249–275.

[66] S. Azizian, *J. Colloid Interface Sci.* **2004**, *276*, 47–52.

[67] J.-P. Simonin, *Chem. Eng. J.* **2016**, *300*, 254–263.

[68] H. Yuh-Shan, *Scientometrics* **2004**, *59*, 171–177.

[69] E. C. Lima, A. A. Gomes, H. N. Tran, *J. Mol. Liq.* **2020**, *311*, 113315.

[70] K. Varani, S. Gessi, S. Merighi, P. A. Borea, in *Thermodynamics and Kinetics of Drug Binding*, John Wiley & Sons, Ltd, **2015**, pp. 15–35.

Manuscript received: July 31, 2023